

Composite Flux-Line Lattices Stabilized in Superconducting Films by a Regular Array of Artificial Defects

M. Baert,¹ V. V. Metlushko,¹ R. Jonckheere,² V. V. Moshchalkov,¹ and Y. Bruynseraede¹

¹Laboratorium voor Vaste-Stoffysika en Magnetisme, Katholieke Universiteit Leuven, B-3001 Leuven, Belgium

²Interuniversity Micro-Electronics Center, Kapeldreef 75, B-3001 Leuven, Belgium

(Received 3 October 1995)

Flux creep rate and critical current have been measured in superconducting Pb/Ge multilayers with a square lattice of submicron holes. The new composite flux-line lattices consisting of single or multi-quantum vortices at holes and single vortices at interstitial positions have been identified. The “metallic” behavior of the flux lines at the interstices at temperatures close to the critical temperature leads to a first-order phase transition analogous to the Mott insulator-metal transition for flux lines, introduced by Nelson and Vinokur.

PACS numbers: 74.60.Ge, 74.25.Ha, 74.76.Db

The response of the flux lines (FL's) in superconductors to the presence of artificial pinning centers is a challenging problem of scientific [1–5] and technological [6] interest. The “flux matter” subjected to the action of thermal fluctuations and random or correlated pinning potential is characterized by a variety of new phases, including the vortex glass, Bose glass, and the entangled flux liquid [7]. These new phases are strongly influenced by *the type of artificial pinning center*. Especially *random arrays* of point defects [8–10] (“random point disorder”) and columnar (“correlated disorder”) defects [1,2] have been intensively studied. The latter are convenient pins to localize the FL and enhance the critical current density J_c if the applied field \vec{H} coincides with that of the irradiation-induced columnar tracks [1].

In spite of progress in understanding the behavior of flux matter in the presence of columnar pins, the *regular arrays* of well-characterized pinning centers are much less studied [4,5]. One of the most efficient and easiest ways to produce such centers in thin films is to make submicron holes [4,5] using lithographic techniques [11–13]. In this case the well-defined periodic pinning potential is formed by the holes with the radius r_h much smaller than the period d of the array. The opposite limit ($r_h \sim d$) has been studied before in superconducting networks [14–16]. The present Letter will focus on perforated films with $r_h \ll d$, which show remarkable “resonant” enhancement of the critical current at well-defined “matching” field when the “attempted” period of the FL lattice a_v coincide with the period d of a regular pinning array and the “attempted” number of FL per hole, n_v , is an integer [4,5,12,13].

A hole of radius r_h can trap at least one FL [17–19]. If the holes are sufficiently large, they can pin multi-quantum vortices [19] with the number of the flux quanta n_v up to a *saturation number* $n_s \cong r_h/2\xi(T)$ [17]. Here $\xi(T)$ is the temperature dependent coherence length. For the FL with $n_v > n_s$ the hole acts as a repulsive center. Because of this saturation effect, the composite flux lattice in fields corresponding to $n_v > n_s$ is expected

to consist of FL pinned at holes (strong pinning) as well as at the interstices (weak pinning), as has been shown theoretically [18].

In all previous studies the commensurability effects between the flux lattice and the regular arrays of holes have only been investigated by measuring the transport critical current density J_c as a function of the magnetic field [4,5]. However, a better way of distinguishing the FL trapped at holes and interstices is to perform magnetization *flux creep* measurements, since one may expect an *important difference in the mobility of FL at holes and at interstices* [18]. To our knowledge a study of flux dynamics in superconducting films with regular array of small ($r_h \ll d$) well-defined pinning centers has not yet been performed, though ac magnetization measurements have been performed for superconducting networks $r_h \sim d$ [20], which are quite different from the limit $r_h \ll d$.

In this Letter we report on measurements of the flux creep rate $S(= d \ln M / d \ln t)$ and J_c in superconducting Pb/Ge multilayers with a square lattice of submicron holes ($r_h = 0.15 \mu\text{m}$). Both S and J_c were derived from magnetization measurements $M(H)$, with the magnetic field perpendicular to the film surface. A very sharp reentrant increase of S is observed in the field corresponding to the penetration of the FL into interstices. By comparing the flux creep anomalies with pronounced peaks in the $J_c(H)$ curves, occurring exactly at the matching fields (H_1, H_2, H_3, \dots), we are able to identify the new composite FL lattices. In agreement with the variation of the saturation number n_s with temperature, we also observed the shift of the onset of the FL penetration into interstices from $H_1 < H < H_2$ ($n_s = 1, T = 6.5 \text{ K}$) to $H_2 < H < H_3$ ($n_s = 2, T = 6 \text{ K}$). Finally, near T_c where the mobility of the FL at interstices is very high, we observed an extremely sharp first-order phase transition in the magnetization $M(H)$, in analogy to Mott's insulator-metal transition for the FL as introduced by Nelson and Vinokur [7].

Besides square lattices of holes described here, we have obtained very similar matching effects for triangular lattices [21]. This proves that in superconducting films

with the antidot lattice $r_h \ll d$, the imposed artificial pinning potential is much larger than the difference between elastic energies for a square and a triangular FL lattice in homogeneous unperforated superconductors.

The Pb/Ge multilayers have been preferred to ordinary films, since these multilayers are type-II superconductors for any total thickness of Pb, provided that in the Pb/Ge multilayer the thickness of the individual Pb layers is sufficiently small. The single Pb films, however, are type-I superconductors when they are thicker than 1600 Å [22]. For thinner Pb films similar matching phenomena could also be observed. It should also be noted that the Pb/Ge multilayers can be further used to study the flux dynamics in dependence upon the coupling strength between superconducting layers varied via the change of the Ge layer thickness.

The high quality Pb/Ge multilayers are prepared in a molecular-beam-epitaxy system and a detailed description of the sample preparation can be found in Ref. [23]. All Pb/Ge samples have a $[\text{Pb}(150 \text{ \AA})/\text{Ge}(140 \text{ \AA})]_3\text{Ge}$ structure, where 3 denotes the number of bilayers and the top film is always a 140 Å thick protective Ge layer. The superconducting transition temperature of the multilayers is $T_c \approx 6.9 \text{ K}$. For our Pb/Ge multilayers, $\lambda(0)$ and $\xi(0)$ can be evaluated using the dirty limit expressions $\xi(0) = (\xi_0 l)^{1/2}$ and $\lambda(0) = \lambda_0(\xi_0/l)^{1/2}$, where $\xi_0 = 830 \text{ \AA}$ and $\lambda_0 = 370 \text{ \AA}$ are the clean limit coherence length and penetration depth of Pb [24] and l is the mean free path. From the measured upper critical field $H_{c2}(0)$ we find that $\xi(0) \approx 120 \text{ \AA}$ and therefore $l \approx 17 \text{ \AA}$ and $\lambda(0) = 2600 \text{ \AA}$.

The well defined lattice of holes ($d = 1 \mu\text{m}$, $r \approx 0.15 \mu\text{m}$) is obtained by a standard lift-off procedure [25]. An atomic force microscopy (AFM) study was performed which revealed surface roughness between the holes less than 10 Å (see Fig. 4 below). The very low surface roughness between the holes ensures that the superconducting properties will mainly be influenced by the presence of the holes. For $d = 1 \mu\text{m}$ the matching fields are $H_n = n \times \phi_0/d^2 = n \times 20.7 \text{ G}$, where n is an integer.

Magnetization measurements were performed in a commercial Quantum Design SQUID magnetometer with a scan length of 3 cm, corresponding to a field homogeneity better than 0.05%. The flux creep rate was measured in the regime of remanent magnetization at fixed temperature with a characteristic time delay of 100 s before the first measurement. We assume that the $J_c(H)$ value is proportional to the width of the $M(H)$ hysteresis loop. The validity of this assumption has also been checked by direct comparison of $J_c(H)$ calculated from $M(H)$ and $J_c(H)$ found from dc transport measurements.

Figure 1 shows the magnetization $M(H)$ data in the perforated multilayer at a temperature very close to T_c . A remarkably sharp drop in $M(H)$ at the first matching field H_1 is clearly observed (note that the distance between the neighboring data points is only $\Delta H = 0.1 \text{ G}$). The

presence of weaker extra peaks at $H < H_1$ is an indication of the fractional flux phases stabilized by the periodic array [12]. In order to analyze these results, we will reply on the saturation number n_s and the pinning potential at interstices U_{pi} [18]. At $T = 6.8 \text{ K}$, $n_s = 1$ and only one FL is attracted to the hole while the second FL is repelled. This situation can be described by the Bose analog of the Mott-Hubbard model for correlated electrons [26]. Since the pinning potential $U_{\text{pi}} \propto d/\lambda(T) \rightarrow 0$ at $T \rightarrow T_c$ [18], the FL repelled by the holes are not localized, and they move freely between different very shallow U_{pi} minima at interstitial positions.

The motion of a very small number of excessive FL at $H > H_1$ leads to a sharp field-induced *first-order phase transition from fully localized FL at $H < H_1$ ("insulator") to a collective delocalized state at $H > H_1$ ("metal")* when the motion of "excessive" FL causes an effective delocalization of all the FL trapped by holes. The main features of this transition correspond to the Mott metal-insulator transition for the FL [7]. It should be noted that previously the existence of the temperature-induced first-order transition was derived from resistivity [27] and magnetization measurements [28], in high-quality high- T_c single crystals.

The evaluation of parameters B^* and T^* [7] shows that in our samples with $r_h > \sqrt{2}\xi$, B^* is very close to the first matching field $B^* \approx B_1 \approx B_\phi$ and T^* is smaller than T_c only by a few mK. In this case the Mott insulator line B_ϕ terminates at temperatures extremely close to T_c , where the relaxation times are very short and therefore the Mott insulator can be observed. As the temperature goes down, the relaxation times increase and the $M(B)$ anomaly

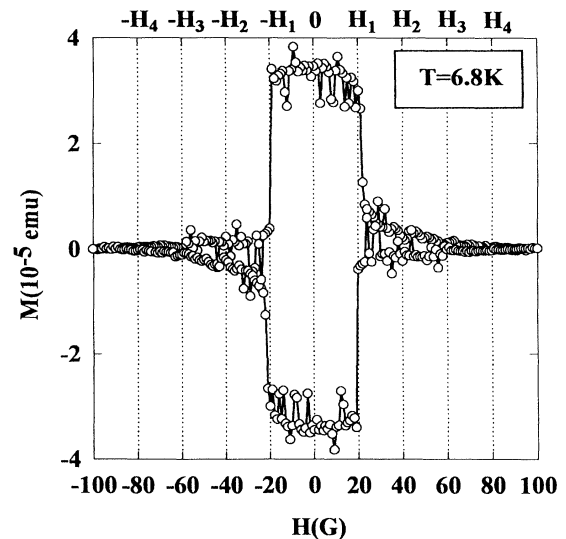


FIG. 1. Magnetization loop $M(H)$ at $T = 6.8 \text{ K}$ of a square lattice of submicron holes ($d = 1 \mu\text{m}$, $r \approx 0.15 \mu\text{m}$). The loops (see also Figs. 3 and 4) were measured for $M > 0$ and symmetrized for clarity for $M < 0$.

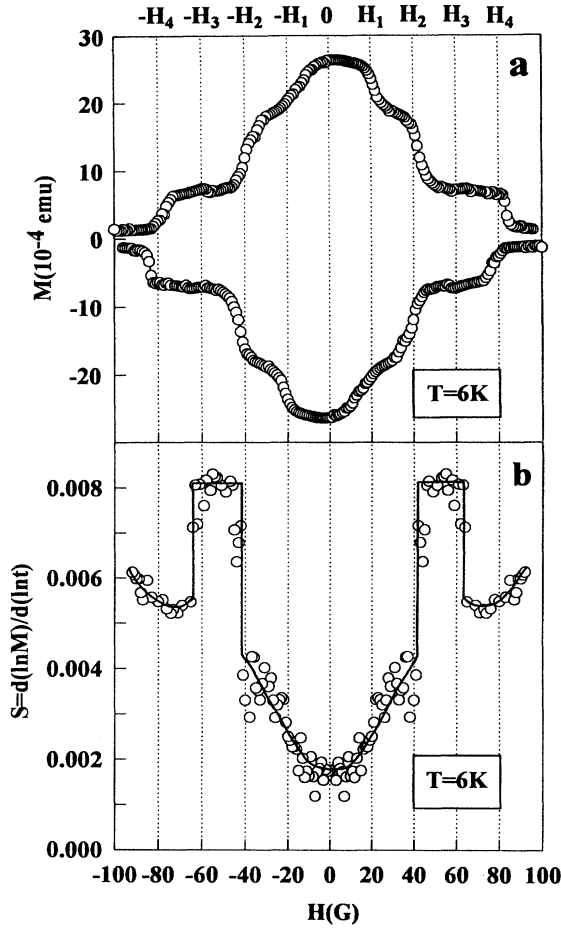


FIG. 2. Magnetization loop $M(H)$ (a) and relaxation rate $S(H)$ (b) at $T = 6$ K of the same multilayer as in Fig. 3. Solid lines are guides to the eye.

at B_1 is suppressed (Fig. 2) due to the equilibrium time problems. Another possibility is that there is no disorder-localized Bose-glass phase at all, sandwiched between the superfluid and the Mott insulator, as shown by numerical simulations [29].

At lower temperature (Fig. 3) we still have $n_s = 1$, but the pinning potential U_{pi} increases substantially and enables one to localize FL at interstices. For fields $H > H_1$, FL are pushed into interstitial positions which is confined by the simultaneous observation of the steplike anomaly in the $M(H)$ curve at $H = H_1$ [Fig. 3(a)] and an abrupt increase of the flux creep rate also at $H = H_1$ [Fig. 3(b)]. In the field range $H_1 < H < H_2$ the increasing S value corresponds to FL loosely bound at interstices. The interstitial positions are completely occupied at $H = H_2$, and a reentrant flux creep rate anomaly shows up indicating the onset of a strongly reduced mobility of the FL. This reduction of mobility signals the onset of the formation of doubly quantized

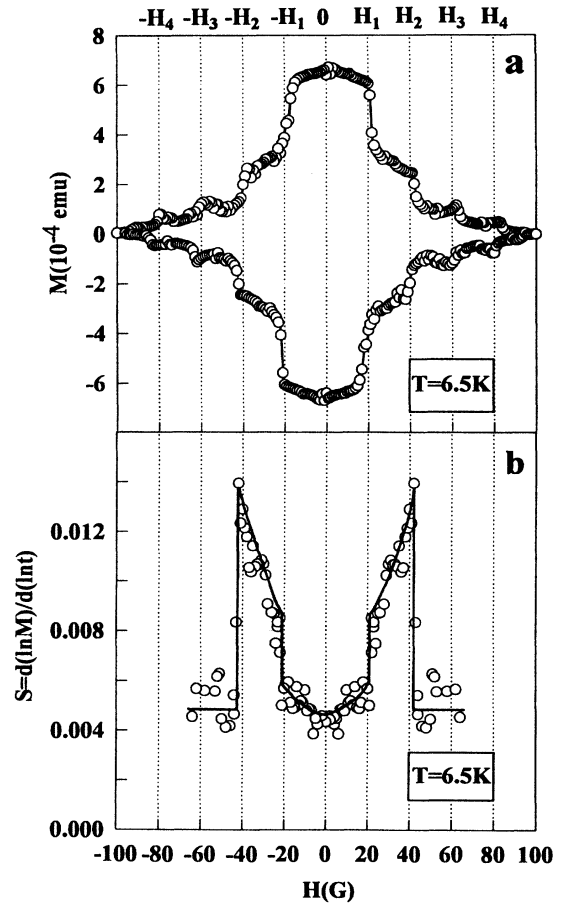


FIG. 3. Magnetization loop $M(H)$ (a) and normalized relaxation rate $S(H)$ (b) at $T = 6.5$ K of a $[\text{Pb}(150 \text{ \AA})/\text{Ge}(140 \text{ \AA})]_3$ multilayer with a square lattice of submicrometer holes ($d = 1 \mu\text{m}$, $r \approx 0.15 \mu\text{m}$). Solid lines are guides to the eye.

vortices at holes, as shown in Fig. 4. Because of the presence of interstitial vortices the saturation value n_s is expected to increase. This leads to the formation of two-quanta vortices at the holes at H_3 (Fig. 4).

We have interpreted the reentrant appearance of the enhanced flux creep rate $S(H)$ at $H_1 < H < H_2$ at $T = 6.5$ K [see Fig. 3(b)] as a consequence of the weak FL pinning at interstitial positions (Fig. 4). If this interpretation is correct, then the temperature-induced change of the saturation number from $n_s = 1$ ($T = 6.5$ K) to $n_s = 2$ ($T = 6$ K) should result in a shift of this reentrant $S(H)$ anomaly from $H_1 < H < H_2$ ($n_s = 1$) to $H_2 < H < H_3$ ($n_s = 2$). This is fully confirmed by decreasing $\xi(T)$ [$n_s \cong r_h/2\xi(T)$] via lowering the temperature down to 6 K. The shape of the $M(H)$ [Fig. 2(a)] and $S(H)$ [Fig. 2(b)] curves convincingly demonstrates the shift of the flux creep rate in the field range $H_2 < H < H_3$ can be interpreted as a result of the existence of mobile FL at interstitial positions.

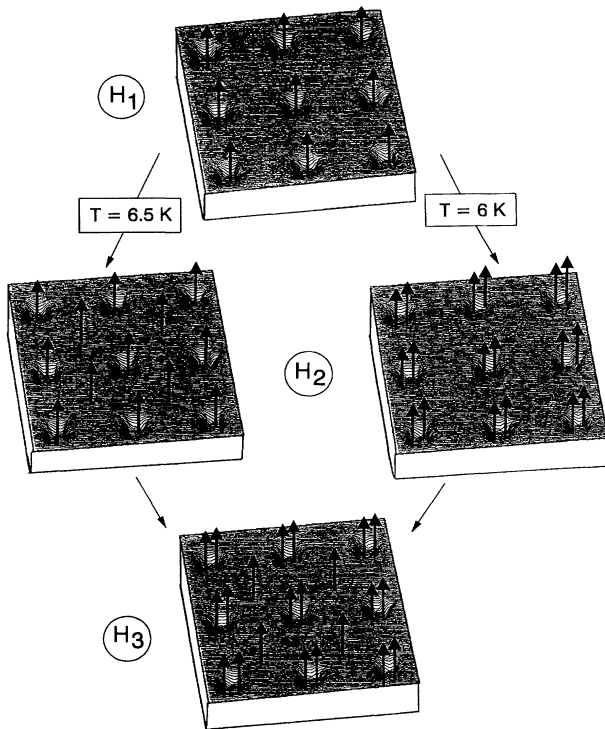


FIG. 4. Schematic presentation of the evolution of the flux-line lattice (arrows) as a function of temperature in a $[\text{Pb}(150 \text{ \AA})/\text{Ge}(140 \text{ \AA})]_3$ multilayer with a square lattice of holes. The AFM pictures used for this presentation clearly show the periodicity of the lattice $d = 1 \mu\text{m}$ and the shape of the holes with $r \approx 0.15 \mu\text{m}$.

The corresponding evolution of the FL lattices at 6.5 and 6 K is shown in Fig. 4. Comparing the $M(H)$ and $S(H)$ data taken at $T = 6.5 \text{ K}$ ($n_s = 1$) and $T = 6 \text{ K}$ ($n_s = 2$) we clearly see that in the first case the penetration of the FL at the interstices is followed by the formation of the two-quanta vortices at holes. In contrast to that in the second case ($T = 6 \text{ K}$) two-quanta vortices are formed before the onset of FL penetration at the interstitial positions. Both scenarios (Fig. 4) lead to the same composite flux lattice at H_3 , but this state is formed via different intermediate states at H_2 .

In conclusion, our data prove that periodic arrays of submicron holes can be successfully used to stabilize composite flux phases consisting of FL sublattices (single or multi-quanta) pinned at holes and at interstitial positions. The mobility of the FL at the interstices is strongly temperature dependent, which makes it possible by tuning the temperature to observe either “metallic” or localized “insulating” behavior of these FL. The “metallic” behavior of the FL at interstices at $T \rightarrow T_c$ leads to a first-order

phase transition at $H = H_1$ which can be treated as an analog of the Mott insulator-metal transition for FL [7].

This work is supported by the Belgian High Temperature Superconductivity Incentive and Concerted Action Programs. The authors are thankful to M. Van Bael and L. Stockman for the AFM and SEM measurements. We also acknowledge useful discussions with K. Temst and C. Van Haesendonck. M. Baert is a Research Fellow of the Belgian Institute for the Encouragement of Scientific Research in Industry and Agriculture. V. V. Metlushko is a Postdoctoral Fellow supported by the University of Leuven.

-
- [1] L. Civale *et al.*, Phys. Rev. Lett. **67**, 648 (1991).
 - [2] W. Gerhäuser *et al.*, Phys. Rev. Lett. **68**, 879 (1992).
 - [3] O. Daldini *et al.*, Phys. Rev. Lett. **32**, 218 (1974).
 - [4] A. F. Hebard, A. T. Fiory, and S. Somekh, IEEE Trans. Magn. **1**, 589 (1977).
 - [5] A. N. Lykov, Solid State Commun. **86**, 531 (1993).
 - [6] J. E. Tkaczyk *et al.*, Appl. Phys. Lett. **62**, 3031 (1993); L. D. Cooley *et al.*, Appl. Phys. Lett. **64**, 1298 (1994).
 - [7] D. R. Nelson and V. M. Vinokur, Phys. Rev. B **48**, 13 060 (1993).
 - [8] L. Civale *et al.*, Phys. Rev. Lett. **65**, 1164 (1990).
 - [9] R. B. van Dover, Appl. Phys. Lett. **56**, 2681 (1990).
 - [10] W. Gerhäuser *et al.*, Physica (Amsterdam) **185C**, 2273 (1991).
 - [11] G. J. Dolan and J. H. Dunsmuir, Physica (Amsterdam) **152B**, 7 (1988).
 - [12] V. V. Moshchalkov *et al.*, Phys. Scr. **T55**, 168 (1994).
 - [13] V. V. Metlushko *et al.*, Solid State Commun. **91**, 331 (1994).
 - [14] B. Pannetier *et al.*, Phys. Rev. Lett. **53**, 1845 (1984).
 - [15] H. S. J. van der Zant, J. Low Temp. Phys. **79**, 289 (1990).
 - [16] R. Théron *et al.*, Phys. Rev. Lett. **71**, 1246 (1993).
 - [17] G. S. Mkrtchyan and V. V. Shmidt, Sov. Phys. JETP **34**, 195 (1972).
 - [18] I. B. Khal'fin and B. Ya. Shapiro, Physica (Amsterdam) **207C**, 359 (1993).
 - [19] A. I. Buzdin, Phys. Rev. B **47**, 11 416 (1993).
 - [20] P. Gandit *et al.*, Physica (Amsterdam) **152B**, 32 (1988).
 - [21] V. V. Moshchalkov *et al.* (to be published).
 - [22] G. J. Dolan, J. Low. Temp. Phys. **15**, 133 (1974).
 - [23] Y. Bruynseraede *et al.*, Phys. Scr. **T42**, 37 (1992).
 - [24] P. G. de Gennes, *Superconductivity of Metals and Alloys* (Addison-Wesley, New York, 1966).
 - [25] K. Temst *et al.*, (to be published).
 - [26] N. E. Mott and E. A. Davis, *Electronic Processes in Non-Crystalline Materials* (Clarendon Press, Oxford, 1979).
 - [27] W. K. Kwok *et al.*, Phys. Rev. Lett. **72**, 1092 (1994).
 - [28] H. Pastoriza *et al.*, Phys. Rev. Lett. **72**, 2951 (1994).
 - [29] W. Krauth, N. Trivedi, and D. Ceperley, Phys. Rev. Lett. **67**, 2307 (1991).